

## Supplementary Information

### Evidence of Strong Spin-orbit coupling in a Gd<sub>2</sub> di-nuclear molecular polymer

Thilini Ekanayaka,<sup>1</sup> Tao Jiang,<sup>2</sup> Emilie Delahaye,<sup>3</sup> Olivier Perez,<sup>4</sup> Jean-Pascal Sutter,<sup>3</sup> Duy Le,<sup>2</sup> Alpha T. N'Diaye,<sup>5</sup> Robert Streubel,<sup>1</sup> Talat S. Rahman,<sup>2</sup> Peter A. Dowben<sup>1</sup>

1. Department of Physics and Astronomy, Theodore Jorgensen Hall, 855 North 16<sup>th</sup> Street, University of Nebraska-Lincoln, Lincoln, NE 68588-0299, United States.
2. Department of Physics, University of Central Florida, 4000 Central Florida Blvd. Building 121 PS 430, Orlando, FL 32816, United States.
3. Laboratoire de Chimie de Coordination du CNRS (LCC), Université de Toulouse, CNRS, Toulouse, France.
4. Normandie Univ, ENSICAEN, Unicaen, CNRS, CRISMAT, 14000 Caen, France
5. Lawrence Berkeley National Laboratory, Advanced Light Source, Berkeley CA 94720, United States.

### Crystal structure

An accurate crystal structure analysis of the [Gd<sub>2</sub>(L)<sub>2</sub>(ox)<sub>2</sub>(H<sub>2</sub>O)<sub>2</sub>] compound is described in this part. Different micrometric crystals were extracted from the batch synthesis and tested with our Synergy S single crystal diffractometer. The choice of samples was crucial for the continuation of the study; the crystals are platelet-shaped and the search for sufficiently thick is often compromised because of the stacking of several individual platelets. The best diffracting samples were selected for further analysis. The preliminary diffraction experiments revealed a triclinic cell characterized by the following cell parameters:  $a = 8.32 \text{ \AA}$ ,  $b = 9.33 \text{ \AA}$ ,  $c = 10.13 \text{ \AA}$ ,  $\alpha = 90.26^\circ$ ,  $\beta = 96.63^\circ$  and  $\gamma = 111.41^\circ$ . A first data collection was performed at room temperature with Cu K $\alpha$  radiation; the full Ewald sphere was collected up to a  $\theta$  angle of  $75^\circ$ . The data reduction led to an internal reliability ( $R_{\text{int}}$ ) factor of 6.8 %, a completeness of 99.7 % and 2837 independent reflections with  $I \geq 3\sigma(I)$ . The cell parameters were:  $a = 8.3223(3) \text{ \AA}$ ,  $b = 9.3130(3) \text{ \AA}$ ,  $c = 10.1369(3) \text{ \AA}$ ,  $\alpha = 90.217(3)^\circ$ ,  $\beta = 96.611(3)^\circ$  and  $\gamma = 111.381(3)^\circ$ . The data analysis was done using Olex2, the structure solved using SHELXT with the space group P-1, and the model was then refined using SHELXL.

The final agreement factor was equal to 4.46 % and the refined composition is C<sub>22</sub>H<sub>26</sub>Gd<sub>2</sub>N<sub>4</sub>O<sub>18</sub>. A view of the refined structure is given in the Figure S2a. However, this figure overshadows many of the problems revealed by the refinement of anisotropic Atomic Displacement Parameters, ADPs (see Figure 2b) leading to strongly elongated ellipsoids for numerous atoms. This anomaly could be a clue for acentric crystal. To determine whether the crystal is centrosymmetric or not an analysis of the Wilson statistic was done. The value of  $\langle |E^2 - 1| \rangle = 0.733$  was clearly in favor of a non-centrosymmetric space group. Consequently, the diffraction

data were revisited by choosing the space group P1. However, this did not diminish the ellipsoid elongation for the different ligand atoms. To reject any problem related to the quality of the measured sample, new collections were made on three other crystals but all these data lead to the same results and the same anomalies on ADP. These anomalies can be a consequence of static or dynamic disorder affecting mainly the ligand L. To avoid dynamic disorder, a new data collection with a strategy similar to RT was performed at 120 K. The observed diffraction patterns are very similar to those observed at room temperature; in particular, no additional reflection associated to a new ordering is evidenced. The data reduction led to a very satisfying data set with  $R_{\text{int}} = 3.48\%$ . The acentric P1 space group was chosen for the structure determination and the final result was very close to that obtained at room temperature; the anomaly on the atomic displacement parameters remained. This outcome totally refuted the hypothesis of the existence of a dynamic disorder. The disorder affecting the ligand being static, it was modelled with each atom constituting the ligand occupying two positions. These two positions were determined on the basis of the direction and amplitude of the ellipsoids. Different restraints on the C–C, C–O, C–N and N–N atomic distances and on the planar character of the imidazolium were applied for refinement. Isotropic ADP was assigned to the atoms affected by the disorder; the same ADP are used for each atom of a disordered atomic pair. The resulting crystal structure is described by two Gd, two oxalate ligands, two water molecules and four ligands L (Figure S3). The four L-ligands have a partial occupation, complementary two by two; the sum of their occupations is equal to two. These four ligands are labelled L1a, L1b, L2a and L2b on the Figure S3; their respective occupancies are 0.43/0.57 and 0.52/0.58. The final agreement factor is equal to 3.6 %.

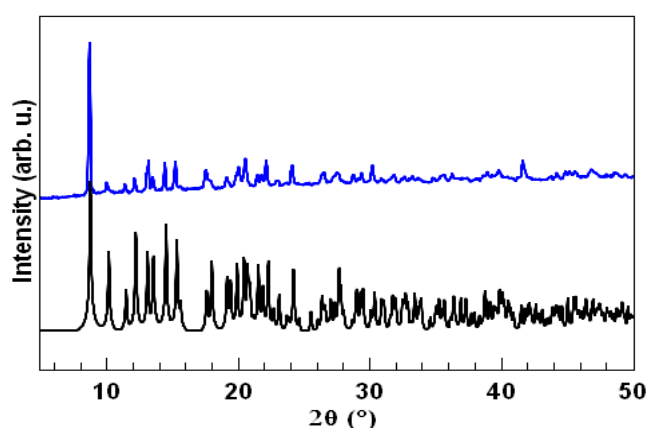


**Figure S1:** Comparison for  $[Gd_2(L)_2(ox)_2(H_2O)_2]$  of the experimental powder X-ray diffraction pattern (blue line) with the calculated pattern from single crystals X-ray data (black line).

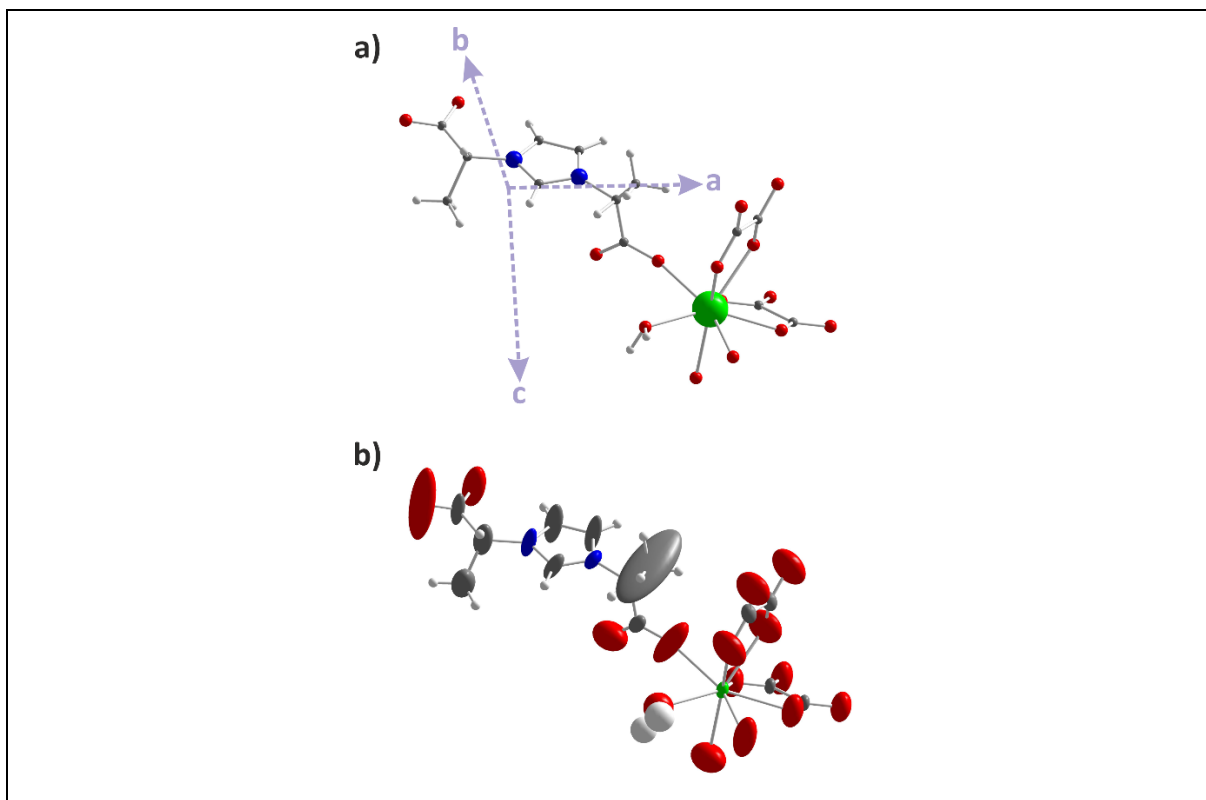


**Figure S2:**  $[Gd(L)(ox)(H_2O)]$  motif determined from single crystal X-ray diffraction data and the space group  $P-1$ . a) Only the atomic position and the crystallographic axes are represented. b) The ellipsoid corresponding to the atomic displacement parameters (ADP) are drawn (at 50 % level?).

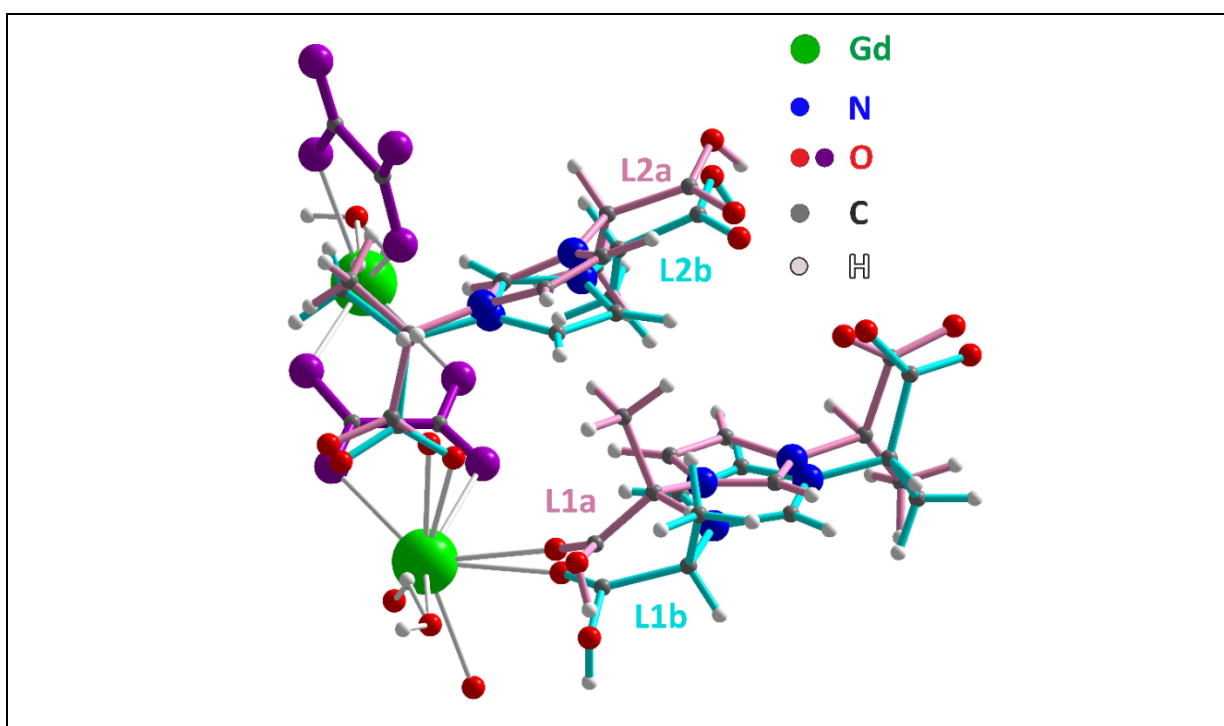


**Figure S3:** View of the motif  $C_{22}H_{26}Gd_2N_4O_{18}$  (e.g.  $[Gd_2(L)_2(ox)_2(H_2O)_2]$ ). The oxalate moieties are colored in purple and the two disordered ligand pairs are drawn in cyan and pink.

Projections of the structure are drawn in the Figure S4; they reveal the 3D organization of the Gd atoms, oxalate and ligand. Gd atoms are surrounded by 8 oxygen atoms ( $2.25\text{\AA} \leq d_{\text{Gd-O}} \leq 2.45\text{\AA}$ ) forming a square antiprismatic coordination sphere with the apexes occupied by four O atoms belonging to oxalate groups, one to a water molecule, and three to carboxylates of two ligands. Each of these polyhedra is isolated but these  $\text{GdO}_8$  units can be considered to be interconnected via oxalate groups; they form  $(\text{GdO}_4\text{-ox}_2)$  infinite chains running along **b** (see Figure S4a and S4b). The ligands ensure the connection between these chains: ligands are connected to two Gd from different chains by their carboxylate groups. Each ligand is bound to one Gd by two O atoms and to the other Gd by only one O. As shown in the Figure S3, the disorder affecting the ligands is quite important and this must be directly related to the existence of a degree of freedom for the rotation of the ligand possibly due to this specific boundary scheme.

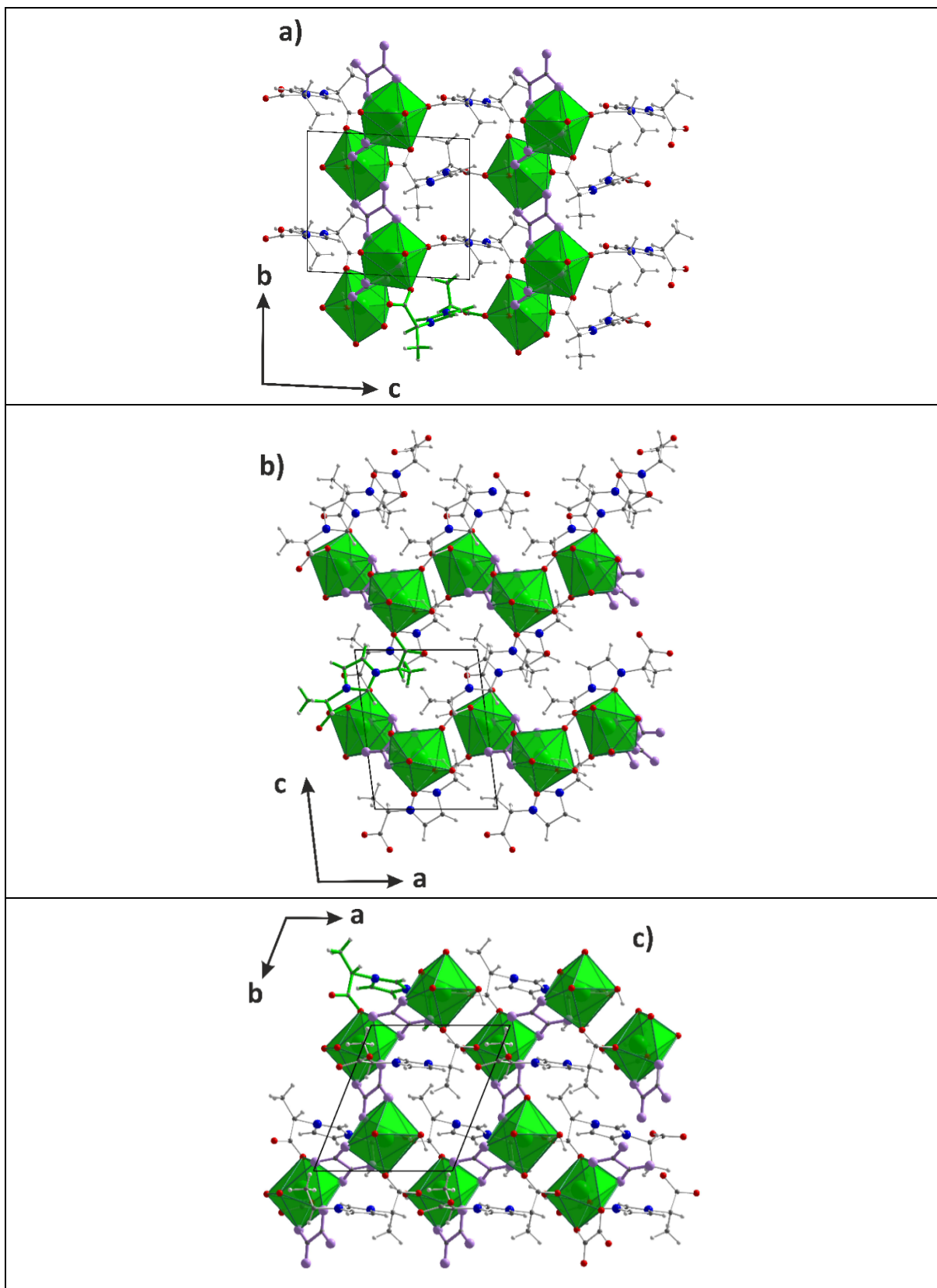


**Figure S4:** Structural projections of the final model of  $[\text{Gd}_2(\text{L})_2(\text{ox})_2(\text{H}_2\text{O})_2]$  along **a** (a), along **b** (b) and along **c** (c). Only the L1a and L2a conformations of the ligands are reported. Oxalate ligands are colored in purple, and the coordination polyhedron is drawn for gadolinium. The internal bonds of one of the ligands have been drawn in green to better visualize the molecule in the different projections.

## Partial Density of States

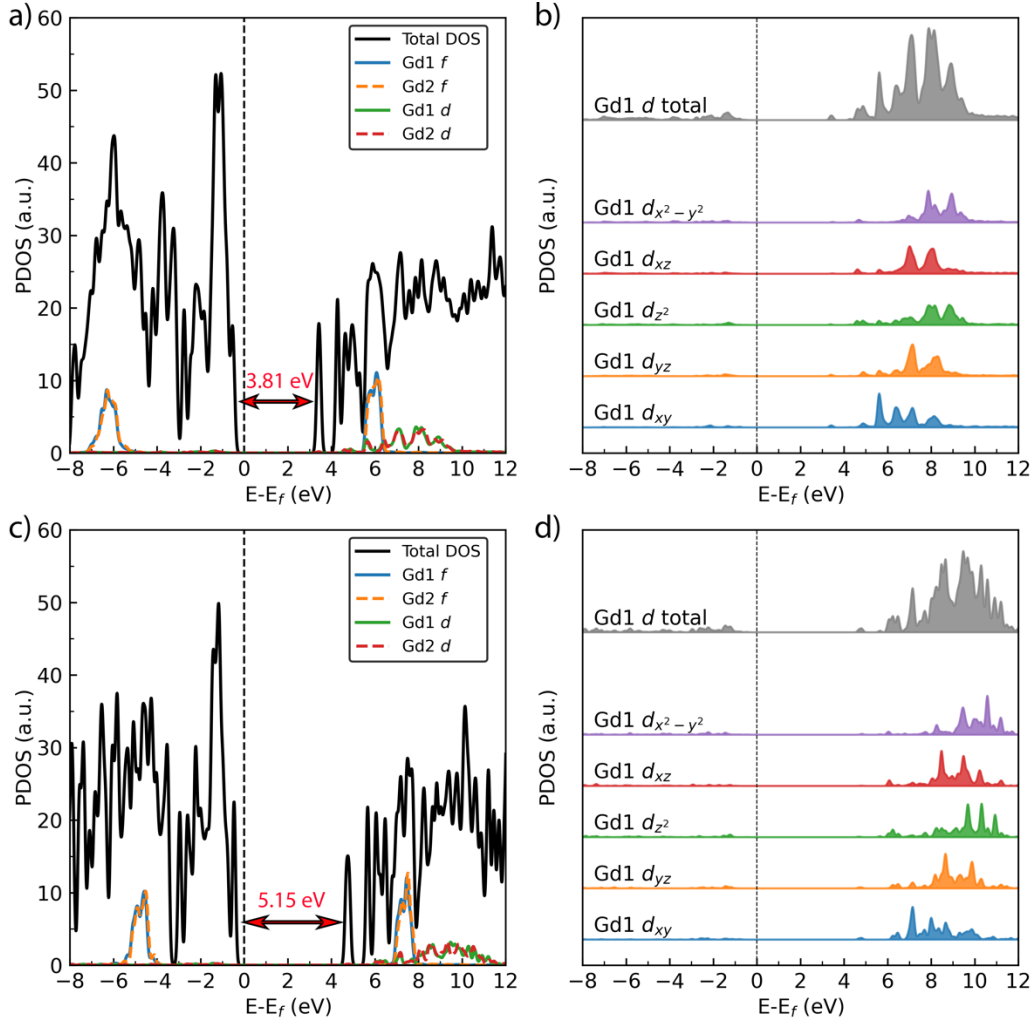


**Figure S5:** Partial Density of States with indicated band gap values of  $[Gd_2(L)_2(ox)_2(H_2O)_2]$  (a) and PDOS of 5d states (b) calculated with PBE+U. (c) and (d) are corresponding data calculated with HSE06 functional.

## Magnetometry

Magnetic measurements were performed with a Quantum Design SQUID-VSM magnetometer (Fig. S6); a magnetic field of 100 Oe was applied to obtain the magnetic susceptibility, and magnetizations was recorded for fields up to 70 kOe. The plot of the product  $\chi_M T$  between 300 and 2 K ( $\chi_M$  stand for the molar susceptibility per  $Gd_2$  moiety and was obtained for  $H = 100$  Oe) shows a constant value down to about 10 K followed by a rapid decrease for lower  $T$  (Fig. S7). In the higher  $T$  domain, the obtained value of  $17.7 \text{ cm}^3 \text{ mol}^{-1} \text{ K}$  is in agreement with the Curie contributions of two independent  $Gd(III)$  with  $S = 7/2$  and this value decreases rapidly below 12 K to reach  $16.1 \text{ cm}^3 \text{ mol}^{-1} \text{ K}$  at 1.8 K. The analysis of  $\chi_M T$  versus  $T$  with the model derived by Fisher<sup>1,2</sup> for an infinite chain of classical spins gave an exchange interaction of  $J_{GdGd}$

$= -(9 \pm 1) \times 10^{-3} \text{ cm}^{-1}$  with Landé factor  $g = 2.12$  according to the expression of the magnetic susceptibility for the Heisenberg model for an infinite chain of exchange coupled spins:

$$\chi = \frac{Ng^2B^2S(S+1)}{3kT} * \frac{1 + \coth\left[\frac{JS(S+1)}{kT}\right] - \frac{kT}{JS(S+1)}}{1 - \coth\left[\frac{JS(S+1)}{kT}\right] - \frac{kT}{JS(S+1)}} \quad (\text{eq. S1})$$

where  $N$  stand for the Avogadro number,  $k$  for the Boltzmann constant,  $B$  for the Bohr magneton,  $S = 7/2$  for  $\text{Gd}^{3+}$ ,  $J$  for the exchange interaction ( $J_{\text{GdGd}}$ ), and  $T$  for the temperature. The variation of  $\chi_M^{-1}$ , measured in the presence of a magnetic bias field (3.5 kOe), is linear over the whole temperature range and Curie-Weiss analysis yielded  $C = 17.7$  and  $\theta = -0.64 \text{ K}$  (Fig. S7, insert), thus confirming the weak antiferromagnetic Gd-Gd interactions. The field dependence of the magnetization recorded at 1.8 K shows no hysteresis opening and a rapid increase for small fields and saturates above 20 kOe with  $14.7 \mu_B$  (Fig. S6 and S7). This behavior also supports the weak interactions between two Gd(III).

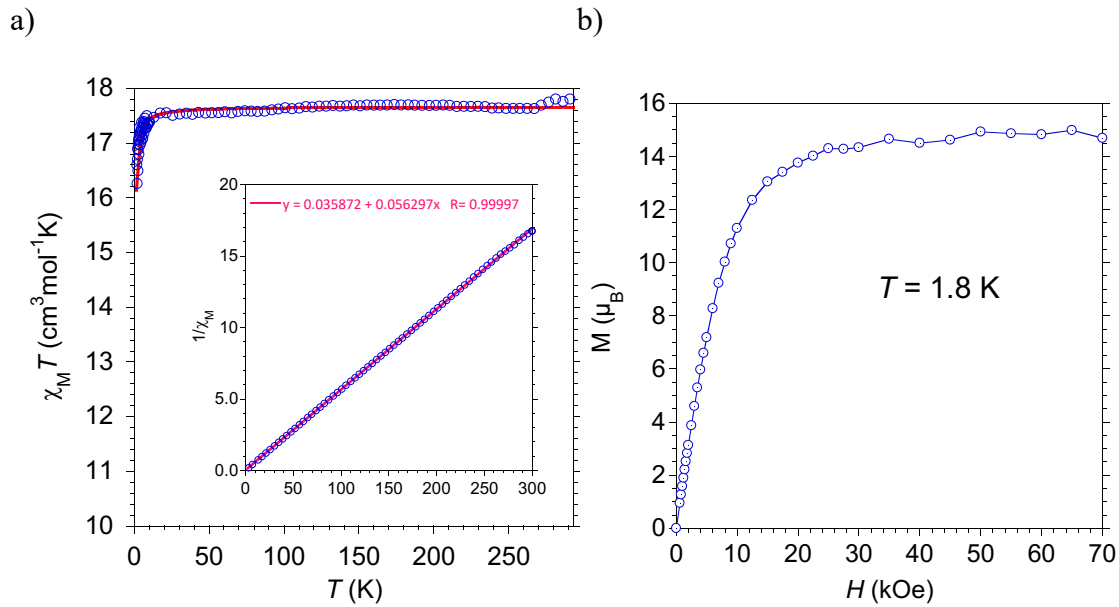


**Figure S6:** The (a) experimental (O) and calculated (—) temperature dependence of the magnetic susceptibility  $\times$  temperature,  $\chi_M \cdot T$ , and (in the insert)  $1/\chi_M$ ; with a linear fit, (b) the field dependence of the magnetization at 1.8 K (the solid line is just a guide to the eye).

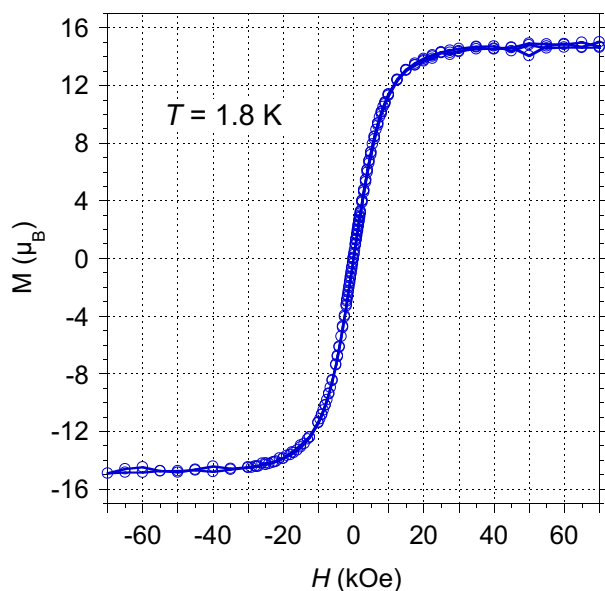


**Figure S7:** Field dependence loop of the magnetization at 1.8 K recorded between 70 and -70 kOe

### Multiplet Fittings of the Gd 5p Core obtained from X-ray photoemission

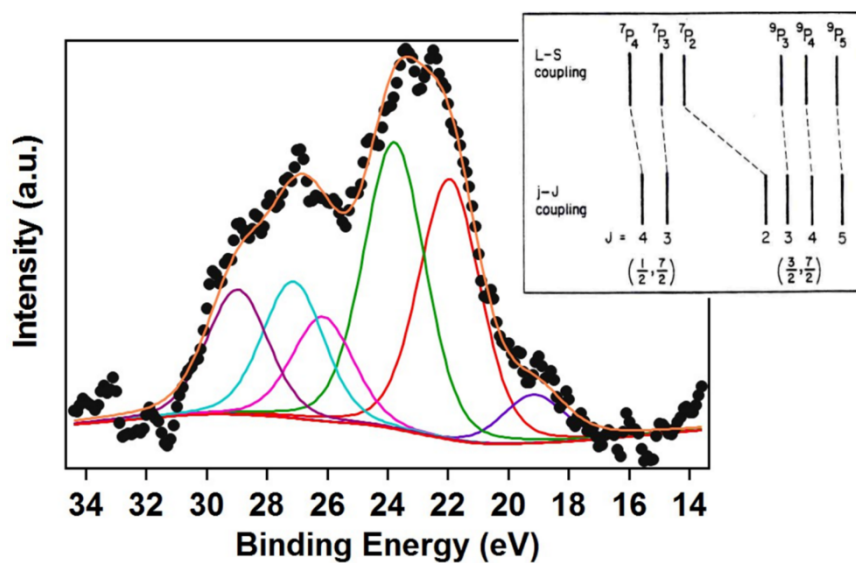


**Figure S8:** The X-ray photoemission spectroscopy of Gd, showing the components of the 5p core level components at binding energies of 19.3 eV, 21.9 eV, 23.7 eV, 26.1 eV, 27.1 eV and 28.9 eV. Binding energies are with respect to the chemical potential (the Fermi level) in terms of  $E_F - E$ .

## References:

<sup>1</sup> Fisher, M. E. Magnetism in One-Dimensional Systems—The Heisenberg Model for Infinite Spin. *American Journal of Physics* **1964**, 32 (5), 343-346. DOI: 10.1119/1.1970340.

<sup>2</sup> Georges, R.; Borras-Almenar, J. J.; Coronado, E.; Curély, J.; Drillon, M. One-dimensional magnetism: An overview of the models. In *Magnetism: Molecules to materials: Models and experiments*, Miller, J.S. and Drillon, M. Ed.; Vol. 1; Wiley-VCH, 2002; pp 1-47.